

# Inorganic Polyphosphate Relieves Ulcerative Colitis by Modulating the Gut Microbiota and Metabolites

Zhicheng Wang, Jing Zhao, Sisi He, Rongpeng Li, Xiuxiu Wang,\* Chao Yan,\* Jing Zhao,\* and Wei Wei\*

Cite This: *ACS Appl. Bio Mater.* 2025, 8, 7473–7480

Read Online

ACCESS |



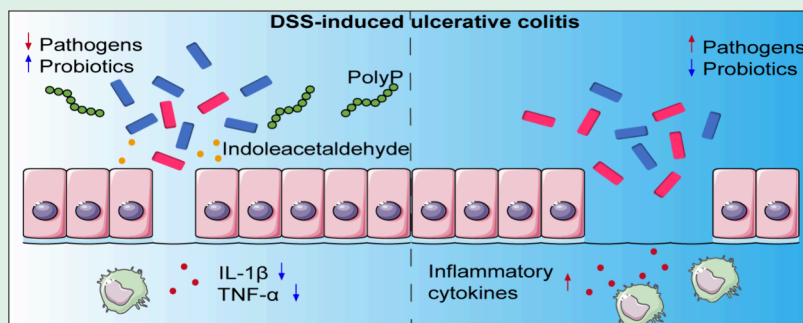
Metrics &amp; More



Article Recommendations



Supporting Information



**ABSTRACT:** Ulcerative colitis (UC) poses a significant therapeutic challenge due to its complex pathogenesis and limited treatment efficacy. Restoring gut microbiota homeostasis is a critical strategy, given its profound influence on immunity and metabolic dysregulation in UC. This study demonstrates the therapeutic potential of inorganic polyphosphate (polyP) in ameliorating UC by modulating gut microbiota and metabolites. *In vivo* experiments demonstrate that polyP administration alleviates colitis pathology, reduces proinflammatory cytokines (IL-1 $\beta$ , TNF- $\alpha$ ), and reinforces intestinal barrier integrity. PolyP restructures microbial communities by enriching probiotics (*Ruminococcaceae*, *Butyrivibrio*, *Blautia*) while depleting *Parasutterella*. Concurrently, it reprograms metabolomic profiles, elevating barrier-repairing metabolites—namely indoleacetaldehyde (IAAld). These findings establish polyP as a microbiota-modulating therapeutic agent for UC, highlighting its role in modeling host-microbiota-metabolite interactions for gut homeostasis.

**KEYWORDS:** Polyphosphate, Biopolymer, Ulcerative colitis, Gut microbiota, Indoleacetaldehyde

## INTRODUCTION

Ulcerative colitis (UC), a prevalent inflammatory bowel disease (IBD), imposes a significant global health burden due to diffuse mucosal inflammation in the colon.<sup>1</sup> Its pathogenesis involves multifactorial interactions, including dysregulated immune responses, gut microbiota alterations, genetic susceptibility, and environmental triggers.<sup>2–4</sup> Notably, UC patients exhibit reduced microbial diversity, diminished probiotics, and enrichment of pathobionts.<sup>5</sup> Emerging evidence underscores that microbiota-derived metabolites, particularly short-chain fatty acids (SCFAs), bile acid derivatives, and amino acid metabolites, serve as critical mediators in UC pathogenesis.<sup>6–9</sup> Hence, elucidating host-microbiota interactions is essential for developing novel UC therapeutics.

Polyphosphate (polyP), a conserved linear polymer of phosphate residues, functions as a key bacterial metabolite regulating energy metabolism, stress adaptation, and metal ion chelation.<sup>10–12</sup> Intriguingly, while Bosmann et al. demonstrated that polyP promotes bacterial immune evasion by polarizing macrophages toward an anti-inflammatory phenotype during sepsis,<sup>13</sup> Fujiya et al. reported its protective role in

UC via platelet aggregation, inflammation reduction, and gut microbiota modulation.<sup>14,15</sup> This functional paradox implies environment-dependent immunomodulation by polyP. Although polyP-induced microbiota remodelling correlates with colitis remission, whether gut microbiota mediate polyP's protective effects through metabolite-driven mechanisms remains elusive. Further investigation into the polyP-microbiota-metabolite axis will advance understanding of both host immunity and the complex biological functions of polyP.

In this study, we demonstrate through *in vivo* experimentation that polyP administration significantly ameliorates UC pathology, reduces pro-inflammatory cytokine expression, and enhances intestinal barrier integrity. Mechanistically, polyP restructures gut microbial communities by enriching probiotics

Received: June 17, 2025

Revised: July 14, 2025

Accepted: July 25, 2025

Published: August 1, 2025



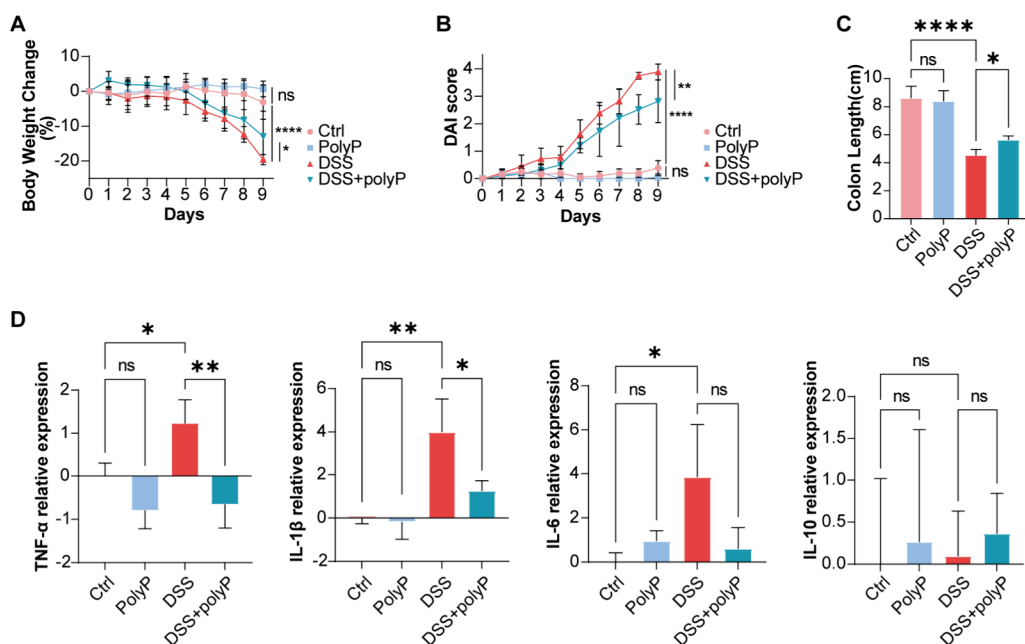


**Figure 1. PolyP treatment ameliorates the colitis *in vivo*.** (A) Average daily body weight change compared to that on Day 0. (B) Average DAI scores. (C) Mouse colon length on Day 9. (D) Log<sub>2</sub> fold change of cytokine mRNA expression relative to the Control group. The data are expressed as the mean  $\pm$  SD ( $n = 3$  or 6).

and drives biosynthesis of barrier-repairing metabolites such as indoleacetaldehyde. These findings establish polyP as a microbiome-modulating agent and provide foundational insights for targeting host-microbiota interactions in UC.

## MATERIALS AND METHODS

**Reagents.** Dextran sulfate sodium (DSS, Mw36,000–50,000) were purchased from MP Biochemicals (Solon, USA). Polyphosphate (polyP) had average length of 100 phosphates and synthesized according to previous methods.<sup>16</sup> One mg polyP was dissolved in 1 mL ddH<sub>2</sub>O, sonicated for 1 min, aliquoted and stored at  $-80^{\circ}\text{C}$  until use. The <sup>31</sup>P NMR spectrum of polyphosphate (polyP) was acquired as shown in Figure S1. The stability of polyP under simulated gastrointestinal conditions was assessed by Urea-PAGE analysis (Figure S2).<sup>17</sup> ArtiCanCEO SYBR qPCR Mix were purchased from Tsingke Biotech (Beijing, China). EZ-10 Total RNA Mini-Preps Kit and MightyScript Plus First Strand cDNA Synthesis Master Mix (gDNA digester) were purchased from Sangon Biotech (Shanghai, China).

**Animals and Experimental Design.** Animal experiments were carried out according to the National Institutes of Health guidelines and the Association for Research in Vision and Ophthalmology guidelines and conducted under the approval of Institutional Animal Care and Use Committee (IACUC) of Nanjing Advanced Academy of Life and Health (AP#: NAALH-N-2412005). Twenty-four specific-pathogen free (SPF) C57BL/6J male mice (5–6 weeks old, 20–22 g) were obtained from Zhejiang Vital River Laboratory Animal Technology Co., Ltd. (Jiaxing, China). After 1 week of adaptation, the mice were randomly divided into 4 groups of 6 mice each: a healthy control group, a PolyP group, a DSS group, and a DSS+PolyP group. To model ulcerative colitis (UC), the mice were given 2.5% DSS to drink freely for 7 days. The mice in the PolyP and DSS+PolyP groups were administered PolyP via gavage daily at a mass-to-mouse body weight ratio of 10 mg/kg, whereas the rest of the mice were given PBS gavage treatment.

Daily measurements of body weight, diarrhea scores and blood stool scores were used to calculate the disease activity index (DAI) following the methods of previous study.<sup>18</sup> On Day 9, the mice were sacrificed to collect colon tissue and faeces for further analysis.

**Histological Analysis.** The colons were rolled and fixed with 4% paraformaldehyde and stained with hematoxylin and eosin (H&E) and Alcian blue and Periodic acid Schiff (AB-PAS). The histological scores and goblet cell counts were performed according to previous studies.<sup>19</sup>

**Real-Time Quantitative Polymerase Chain Reaction Analysis.** Total RNA from colon tissue samples was isolated according to the manufacturer's instructions. Total RNA (1  $\mu\text{g}$ ) was used for cDNA synthesis following the instructions. RT-qPCR analysis was performed according to the instructions of a Step-One Plus RT-qPCR system (Applied Biosystems, USA). Eef2 was used as an internal control to determine the relative expression of the target mRNA in colonic tissues by using the Log<sub>2</sub>(2 <sup>$\Delta\Delta\text{Ct}$</sup> ) method. RT-qPCR primer sequences are provided in Table S1.

**Microbiomics Analysis.** In brief, bacterial total genomic DNA was isolated by using a DNeasy PowerSoil kit (Qiagen, Germany) following the manufacturer's instructions. 16S rRNA sequencing was performed on an Illumina MiSeq platform with a primer set specific to the V3 and V4 regions, and the analysis was conducted by using QIIME 2 and the LEfSe analysis package.

**Metabolomics Analysis.** In brief, faeces were quantified by using untargeted metabolomics based on a liquid chromatography–tandem mass spectrometry (LC–MS/MS) system consisting of a Waters ACQUITY UPLC I-Class plus and Thermo-Obritrapp-QE. The raw data were subjected to metabolomics processing with Progenesis QI v3.0 software (Nonlinear Dynamics, Newcastle, UK). Identification analyses were performed by using the Human Metabolome Database (HMDB), Lipidmaps (v2.3) and METLIN databases.

**Statistical Analysis.** The results were analyzed and plotted by using GraphPad Prism 8 software. All results are expressed as the mean  $\pm$  standard deviation (SD) repeated measurements. The data were analyzed with standard unpaired two-tailed Student's *t* tests and one-way analysis of variance (ANOVA), where applicable. *P*-value  $< 0.05$  was considered to indicate statistical significance. \**P*  $< 0.05$ , \*\**P*  $< 0.01$ , \*\*\**P*  $< 0.001$ , \*\*\*\**P*  $< 0.0001$  and ns means *P*  $> 0.05$ .

## RESULTS AND DISCUSSION

**Polyphosphate Ameliorated Colitis Symptoms in Colitis Mice.** To evaluate polyphosphate (polyP) efficacy in ulcerative colitis (UC), DSS-induced colitis mice received daily

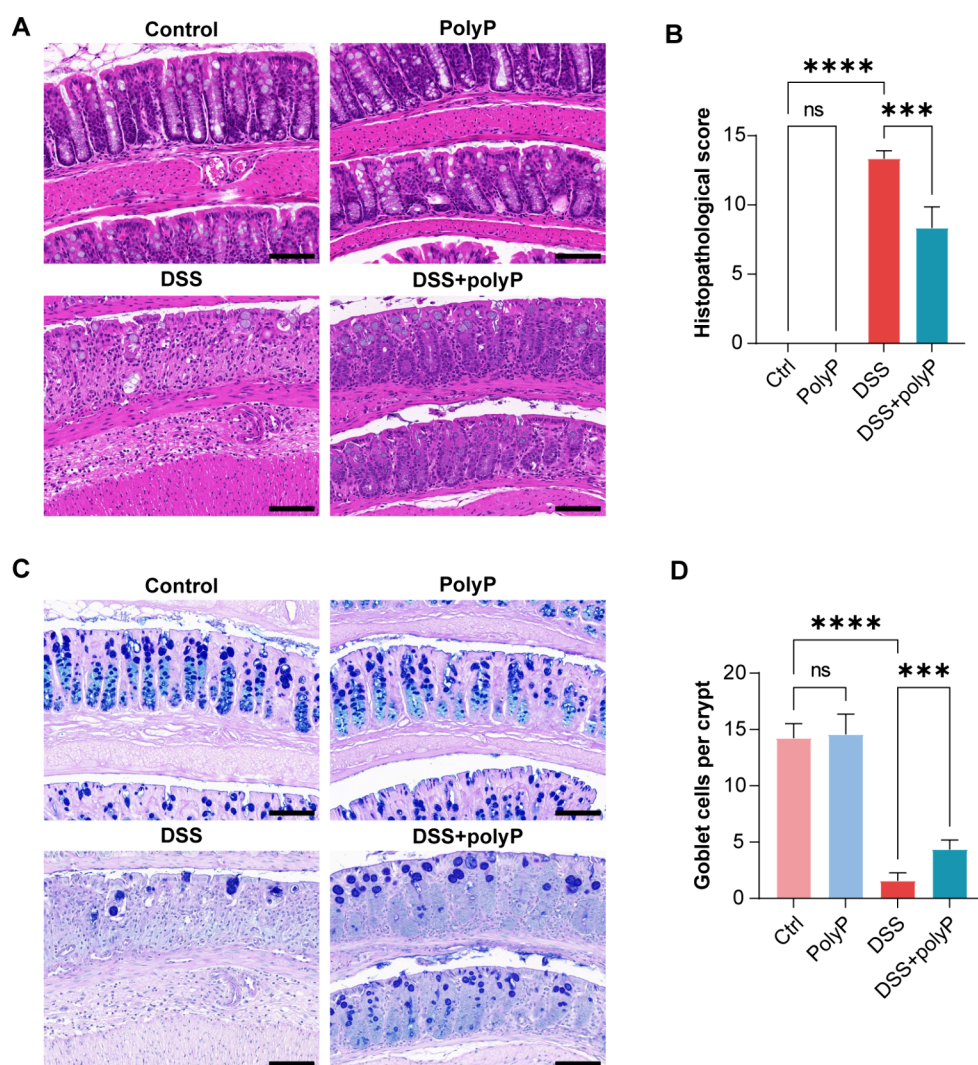


**Figure 2. PolyP treatment reinforces intestinal mucosal barrier.** (A) Typical H&E staining of the colon (scale bars: 50  $\mu$ m). (B) The histopathological score of H&E staining. (C) Typical AB-PAS staining of the colon (scale bars: 50  $\mu$ m). (D) Goblet cells per crypt of the colon. The data are expressed as the mean  $\pm$  SD ( $n = 3$ ).

oral polyP (10 mg/kg body weight) throughout the experimental period. PolyP administration significantly ameliorated disease severity relative to DSS controls, evidenced by increased colon length, restored body weight, and reduced Disease Activity Index (DAI) scores (Figure 1A-C).

Given the pivotal role of inflammatory cytokines in UC pathogenesis, we quantified colonic mRNA expression of key mediators. PolyP treatment significantly suppressed pro-inflammatory cytokines IL-1 $\beta$  and TNF- $\alpha$  compared to DSS group, whereas IL-6 and IL-10 levels remained nonsignificant altered. (Figure 1D). These results demonstrate polyP's capacity to attenuate DSS-induced inflammatory damage.

Given the central role of intestinal barrier dysfunction in UC pathogenesis,<sup>20</sup> we assessed polyP's effects on epithelial integrity. Histological analysis demonstrated that polyP administration significantly mitigated DSS-induced epithelial damage, concomitant with increased goblet cell density versus DSS controls (Figure 2A-D). This restoration of mucosal guardians indicates enhanced barrier protection. Meanwhile, equivalent polyP doses in healthy mice induced no significant alterations in body weight, colon morphology, or histoarchitecture.

### Polyphosphate Altered the Gut Microbiota Composition.

Given the established role of gut microbiota dysbiosis in UC pathogenesis,<sup>9,21–23</sup> we employed 16S rRNA sequencing to investigate polyP-induced gut microbiota alterations. The results of the ACE and Simpson scores demonstrated that the polyP treatment exhibited a tendency to reverse the DSS-induced significant decrease in beta diversity. However, no significant difference in alpha diversity was observed among the three groups (Figure 3A). Principal coordinate analysis (PCoA) confirmed preserved global community structure (Figure 3B), prompting focused analysis of specific strains.

At the phylum level, DSS elicited a marked increase in Proteobacteria with concomitant Bacteroidetes depletion, disrupting the Firmicutes/Bacteroidetes equilibrium. PolyP counteracted this dysbiosis by significantly elevating Firmicutes while suppressing Proteobacteria (Figure 3C). LEfSe analysis identified *Parasutterella*, *Ruminococcaceae*, *Butyrivococcus*, and *Harryflintia* as key biomarkers. Specifically, polyP administration substantially decreased *Parasutterella* abundance while enriching butyrogenic bacteria *Ruminococcaceae* and *Butyrivococcus*, along with *Harryflintia* (Figure 3D, E). *Parasutterella* is a core member of the gut microbiota, playing an important role

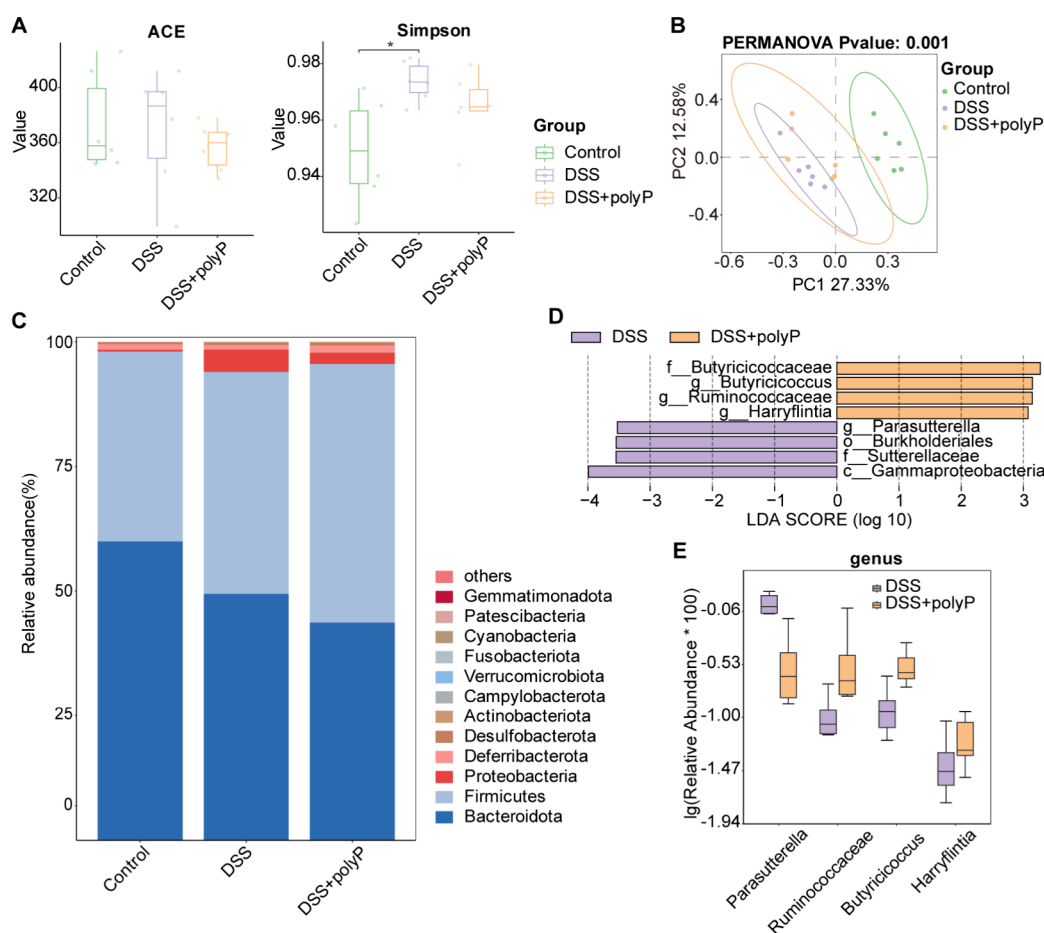


**Figure 3.** PolyP treatment alters the features of the microbiota in colitis mice. (A) The alpha diversity of the gut microbiota according to the ACE and Simpson indices. (B) The beta diversity of the gut microbiota demonstrated by principal coordinate analysis (PCoA). (C) Relative abundance of the gut microbiota at the phylum level. (D) LDA identification of the biomarkers between DSS and DSS+polyP group (LDA score >3). (E) Relative abundance of the significant different gut microbiota at the genus level between DSS and DSS+polyP group ( $n = 6$ ).

in a variety of diseases, including intestinal inflammation and obesity.<sup>24,25</sup> A recent study has revealed that *Parasutterella* plays a significant role in bile acid maintenance and cholesterol metabolism.<sup>26</sup> *Ruminococcaceae* has been identified as a key component of the gut microbiota in IBD, and its levels are known to decrease after the colitis.<sup>27,28</sup> It has been reported to play an important role in the degradation of resistant starch (RS).<sup>29</sup> *Butyricococcus*, which produces the beneficial substance butyrate, has been shown to have a beneficial effect on intestinal mucosal barrier function.<sup>30,31</sup> Butyrate is a type of SCFA that is primarily metabolized by Firmicutes. It is recognized for its pivotal function in maintaining intestinal barrier function, modulating immune responses and anti-inflammation.<sup>32,33</sup> Although the function of *Harryflintia* remains unknown, it has been reported that LPS results in a significant reduction in the relative abundance of *Harryflintia* in mice.<sup>34</sup> Collectively, these polyP-driven microbial dynamics implicate SCFA-mediated mechanisms in barrier restoration.

**Polyphosphate Regulated Gut Microbiota's Metabolites.** Given the critical role of microbial metabolite homeostasis in UC progression,<sup>35,36</sup> we employed untargeted metabolomics to decode polyP's metabolic reprogramming effects. Principal component analysis (PCA) revealed profound DSS-induced metabolic perturbations, whereas the metabolite composition was not significantly altered by the polyP treatment (Figure 4A). The volcano plots showed that 202

metabolites were significantly downregulated and 25 were significantly upregulated in polyP-treated colitis mice (Figure 4B). Notably, polyP specifically upregulated D5-L-Glutamyl-taurine, Urobilin and Indoleacetaldehyde (Figure 4C). Further KEGG pathway analysis revealed that the polyP treatment significantly influenced the Pantothenate and CoA biosynthesis and Taurine and Hypotaurine Metabolism (Figure 4D).

The extant research has demonstrated that there is a significant decrease in both Urobilin and taurine levels in patients with IBD.<sup>37,38</sup> Taurine, a semiessential amino acid, is the end-product of S-L-Glutamyl-taurine, which has functions such as anti-inflammatory, antioxidant, and enhancement of intestinal barrier function.<sup>39,40</sup> Indoleacetaldehyde (IAAld), a key intermediate in the tryptophan metabolic pathway, is further converted into indoleacetic acid (IAA). The multifaceted regulatory function of indoles in IBD is facilitated by the activation of the aryl hydrocarbon receptor (AhR).<sup>41</sup> Activation of the AhR has been demonstrated to inhibit the NF- $\kappa$ B signaling pathway, thereby reducing the release of pro-inflammatory factors and promoting the differentiation of regulatory T-cells.<sup>42</sup> In addition, AhR activation has been shown to up-regulate the expression of tight junction proteins and mucins, thereby enhancing the integrity of the intestinal barrier.<sup>43–45</sup> These coordinated metabolic shifts position polyP as a modulator of microbial indole-AhR axis-driven barrier protection.

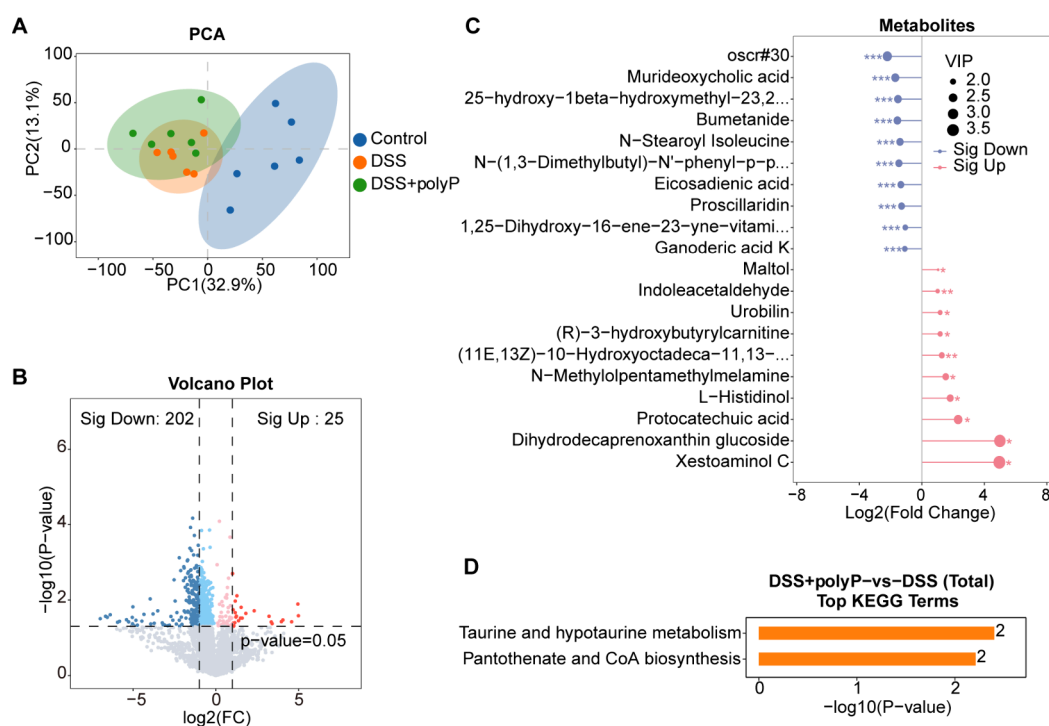


**Figure 4. Untargeted metabolomics of intestinal contents.** (A) Principal component analysis (PCA) based on total metabolites. (B) Volcano plot of the differentially abundant metabolites between the DSS+PolyP group and the DSS group. (C) Lollipopmap of the top 20 differentially abundant metabolites between the DSS+PolyP group and the DSS group. (D) KEGG pathway analysis of differentially abundant metabolites between the DSS+PolyP group and the DSS group ( $n = 6$ )

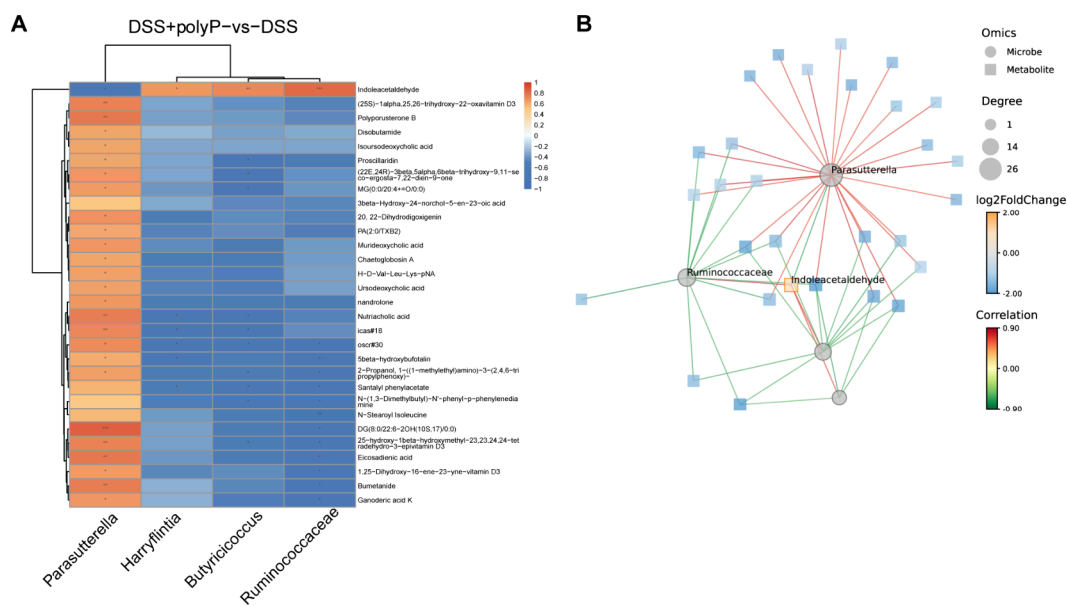


**Figure 5. Indoleacetaldehyde plays a key role in polyP treatment.** (A) Heatmap of the top 30 correlated microbiota at the genus level and metabolites. Red indicates a positive correlation, and blue indicates a negative correlation. (B) Network analysis of significantly correlated microbiota at the genus level and metabolites (filter set:  $p$  value  $< 0.05$ ). The orange line represents a positive correlation, and the green line represents a negative correlation.

**The Relationship between Microbiomics and Metabolomics.** To determine the polyP's mechanism of action, we combined microbiome-metabolome data sets via Spearman correlation analysis. Heatmap visualization of the top 30 differential bacteria and metabolites revealed genus-specific associations. *Parasutterella* exhibited significant positive correlations with 25 metabolites but strong negative

correlation with indoleacetaldehyde (IAald) (Figure 5A). *Ruminococcaceae*, *Harryflintia*, and *Butyricoccus* demonstrated inverse correlation patterns. Crucially, IAald and oscr#30 exhibited a significant correlation with all four bacteria. This interconnectivity was further validated in correlation networks of the top 20 differential features, confirming IAald as a central node linking polyP-modulated bacteria (Figure 5B). Collec-

tively, IAald emerges as a key microbial metabolite biomarker mediating polyP's therapeutic efficacy.

## CONCLUSION

In conclusion, we demonstrated that polyP effectively attenuated colitis and enriched *Ruminococcaceae* and *Butyrivibrio*. Critically, indoleacetaldehyde was identified as a key microbial metabolite biomarker of polyP efficacy. Integrated correlation analyses confirmed interconnected microbial remodeling and metabolite shifts driving disease remission, advancing polyP as a promising microbiota-targeted therapeutic. To directly address the mechanistic limitations identified in this study, future work may employ bacterial transcriptomics to elucidate polyP's specific actions on gut microbes, complemented by fecal microbiota transplantation (FMT) studies to validate causal relationships. Furthermore, rigorously evaluating size-fractionated polyP preparations is critical to overcome the current knowledge gap in chain-length dependency, thereby enabling optimization of therapeutic efficacy for clinical translation.

## ASSOCIATED CONTENT

### Supporting Information

The Supporting Information is available free of charge at <https://pubs.acs.org/doi/10.1021/acsabm.5c01160>.

RT-qPCR primes used in this work;  $^{31}\text{P}$  NMR spectrum of polyP; Urea-PAGE analysis for polyP (PDF)

## AUTHOR INFORMATION

### Corresponding Authors

**Xiuxiu Wang** – State Key Laboratory of Coordination Chemistry, Chemistry and Biomedicine Innovation Center (ChemBIC), School of Life Sciences, Nanjing University, Nanjing 210023, China; School of Chemistry and Chemical Engineering, Nanjing University, Nanjing 210023, China; NJU Xishan Institute of Applied Biotechnology, Wuxi 214000, China; Email: [wangxiuxiu@nju.edu.cn](mailto:wangxiuxiu@nju.edu.cn)

**Chao Yan** – State Key Laboratory of Pharmaceutical Biotechnology, School of Life Sciences, Nanjing University, Nanjing 210023, China; Email: [yanchao@nju.edu.cn](mailto:yanchao@nju.edu.cn)

**Jing Zhao** – State Key Laboratory of Coordination Chemistry, Chemistry and Biomedicine Innovation Center (ChemBIC), School of Life Sciences, Nanjing University, Nanjing 210023, China; School of Chemistry and Chemical Engineering, Nanjing University, Nanjing 210023, China; NJU Xishan Institute of Applied Biotechnology, Wuxi 214000, China; [orcid.org/0000-0001-5177-5699](https://orcid.org/0000-0001-5177-5699); Email: [jingzhao@nju.edu.cn](mailto:jingzhao@nju.edu.cn)

**Wei Wei** – State Key Laboratory of Coordination Chemistry, Chemistry and Biomedicine Innovation Center (ChemBIC), School of Life Sciences, Nanjing University, Nanjing 210023, China; NJU Xishan Institute of Applied Biotechnology, Wuxi 214000, China; [orcid.org/0000-0003-0845-0527](https://orcid.org/0000-0003-0845-0527); Email: [weiwei@nju.edu.cn](mailto:weiwei@nju.edu.cn)

### Authors

**Zhicheng Wang** – State Key Laboratory of Coordination Chemistry, Chemistry and Biomedicine Innovation Center (ChemBIC), School of Life Sciences, Nanjing University, Nanjing 210023, China; State Key Laboratory of Pharmaceutical Biotechnology, School of Life Sciences,

Nanjing University, Nanjing 210023, China; NJU Xishan Institute of Applied Biotechnology, Wuxi 214000, China  
**Jing Zhao** – NJU Xishan Institute of Applied Biotechnology, Wuxi 214000, China

**Sisi He** – Department of Oncology, The Second Affiliated Hospital of Zunyi Medical University, Zunyi 563000, China

**Rongpeng Li** – Medical School of Nantong University, Nantong 226001, China; [orcid.org/0000-0002-8623-9068](https://orcid.org/0000-0002-8623-9068)

Complete contact information is available at: <https://pubs.acs.org/10.1021/acsabm.5c01160>

## Funding

This research was supported by the National Natural Science Foundation of China (22025701 and 22177048), the Natural Science Foundation of Jiangsu Province (BK20232020, BK20220764), the Nanjing Science and Technology Project (202305003), the Fundamental Research Funds for the Central Universities, and the Shenzhen Bay Laboratory Open Fund Project (SZBL2021080601013).

## Notes

The authors declare no competing financial interest.

## ACKNOWLEDGMENTS

We thank OE Biotech Co., Ltd. (Shanghai, China) for providing technological assistance in the omics analysis.

## REFERENCES

- (1) Le Berre, C.; Honap, S.; Peyrin-Biroulet, L. Ulcerative colitis. *Lancet* **2023**, *402* (10401), 571–584.
- (2) Jostins, L.; Ripke, S.; Weersma, R. K.; Duerr, R. H.; McGovern, D. P.; Hui, K. Y.; Lee, J. C.; Philip Schumm, L.; Sharma, Y.; Anderson, C. A.; et al. Host-microbe interactions have shaped the genetic architecture of inflammatory bowel disease. *Nature* **2012**, *491* (7422), 119–124.
- (3) de Lange, K. M.; Moutsianas, L.; Lee, J. C.; Lamb, C. A.; Luo, Y.; Kennedy, N. A.; Jostins, L.; Rice, D. L.; Gutierrez-Achury, J.; Ji, S.-G.; et al. Genome-wide association study implicates immune activation of multiple integrin genes in inflammatory bowel disease. *Nat. Genet.* **2017**, *49* (2), 256–261.
- (4) Piovani, D.; Danese, S.; Peyrin-Biroulet, L.; Nikolopoulos, G. K.; Lytras, T.; Bonovas, S. Environmental Risk Factors for Inflammatory Bowel Diseases: An Umbrella Review of Meta-analyses. *Gastroenterology* **2019**, *157* (3), 647–659.e4.
- (5) Lloyd-Price, J.; Arze, C.; Ananthakrishnan, A. N.; Schirmer, M.; Avila-Pacheco, J.; Poon, T. W.; Andrews, E.; Ajami, N. J.; Bonham, K. S.; Brislawn, C. J.; et al. Multi-omics of the gut microbial ecosystem in inflammatory bowel diseases. *Nature* **2019**, *569* (7758), 655–662.
- (6) Hoque, S. S.; Poxton, I. R.; Ghosh, S. Gut bacteria and ulcerative colitis — A broken tolerance. *Gastroenterology* **2000**, *118* (4), A807.
- (7) Schirmer, M.; Denson, L.; Vlamakis, H.; Franzosa, E. A.; Thomas, S.; Gotman, N. M.; Rufo, P.; Baker, S. S.; Sauer, C.; Markowitz, J.; et al. Compositional and Temporal Changes in the Gut Microbiome of Pediatric Ulcerative Colitis Patients Are Linked to Disease Course. *Cell Host & Microbe* **2018**, *24* (4), 600–610.e4.
- (8) Sinha, S. R.; Haileselassie, Y.; Nguyen, L. P.; Tropini, C.; Wang, M.; Becker, L. S.; Sim, D.; Jarr, K.; Spear, E. T.; Singh, G.; et al. Dysbiosis-Induced Secondary Bile Acid Deficiency Promotes Intestinal Inflammation. *Cell Host & Microbe* **2020**, *27* (4), 659–670.e5.
- (9) Franzosa, E. A.; Sirota-Madi, A.; Avila-Pacheco, J.; Fornelos, N.; Haiser, H. J.; Reinker, S.; Vatanen, T.; Hall, A. B.; Mallick, H.; McIver, L. J.; et al. Gut microbiome structure and metabolic activity in inflammatory bowel disease. *Nature Microbiology* **2019**, *4* (2), 293–305.

- (10) Kim, K.-S.; Rao, N. N.; Fraley, C. D.; Kornberg, A. Inorganic polyphosphate is essential for long-term survival and virulence factors in *Shigella* and *Salmonella* spp. *Proc. Natl. Acad. Sci. U. S. A.* **2002**, *99* (11), 7675–7680.
- (11) Tunpiboonsak, S.; Mongkolrob, R.; Kitudomsub, K.; Thanwatanaying, P.; Kiettipirodom, W.; Tungboontina, Y.; Tungpradabkul, S. Role of a *Burkholderia pseudomallei* polyphosphate kinase in an oxidative stress response, motilities, and biofilm formation. *Journal of Microbiology* **2010**, *48* (1), 63–70.
- (12) Beauvoit, B.; Rigoulet, M.; Raffard, G.; Canioni, P.; Guerin, B. Differential sensitivity of the cellular compartments of *Saccharomyces cerevisiae* to protonophoric uncoupler under fermentative and respiratory energy supply. *Biochemistry* **1991**, *30* (47), 11212–11220.
- (13) Roewe, J.; Stavrides, G.; Strueve, M.; Sharma, A.; Marini, F.; Mann, A.; Smith, S. A.; Kaya, Z.; Strobl, B.; Mueller, M.; et al. Bacterial polyphosphates interfere with the innate host defense to infection. *Nat. Commun.* **2020**, *11* (1), 4035.
- (14) Fujiya, M.; Ueno, N.; Kashima, S.; Tanaka, K.; Sakatani, A.; Ando, K.; Moriichi, K.; Konishi, H.; Kamiyama, N.; Tasaki, Y.; et al. Long-Chain Polyphosphate Is a Potential Agent for Inducing Mucosal Healing of the Colon in Ulcerative Colitis. *Clinical Pharmacology & Therapeutics* **2020**, *107* (2), 452–461.
- (15) Isozaki, S.; Konishi, H.; Fujiya, M.; Tanaka, H.; Murakami, Y.; Kashima, S.; Ando, K.; Ueno, N.; Moriichi, K.; Okumura, T. Probiotic-Derived Polyphosphate Accelerates Intestinal Epithelia Wound Healing through Inducing Platelet-Derived Mediators. *Mediators of Inflammation* **2021**, *2021*, 5582943.
- (16) Ferrucci, V.; Kong, D.-Y.; Asadzadeh, F.; Marrone, L.; Boccia, A.; Siciliano, R.; Criscuolo, G.; Anastasio, C.; Quarantelli, F.; Comegna, M.; et al. Long-chain polyphosphates impair SARS-CoV-2 infection and replication. *Science Signaling* **2021**, *14* (690), No. eabe5040.
- (17) Smith, S. A.; Morrissey, J. H. Sensitive fluorescence detection of polyphosphate in polyacrylamide gels using 4',6-diamidino-2-phenylindol. *ELECTROPHORESIS* **2007**, *28* (19), 3461–3465.
- (18) Zeng, W.; Wu, J.; Xie, H.; Xu, H.; Liang, D.; He, Q.; Yang, X.; Liu, C.; Gong, J.; Zhang, Q.; et al. Enteral nutrition promotes the remission of colitis by gut bacteria-mediated histidine biosynthesis. *eBioMedicine* **2024**, *100*, 104959.
- (19) Kihara, N.; de la Fuente, S. G.; Fujino, K.; Takahashi, T.; Pappas, T. N.; Mantyh, C. R. Vanilloid receptor-1 containing primary sensory neurones mediate dextran sulphate sodium induced colitis in rats. *Gut* **2003**, *52* (5), 713–719.
- (20) Nyström, E. E. L.; Martinez-Abad, B.; Arike, L.; Birchenough, G. M. H.; Nonnecke, E. B.; Castillo, P. A.; Svensson, F.; Bevens, C. L.; Hansson, G. C.; Johansson, M. E. V. An intercrypt subpopulation of goblet cells is essential for colonic mucus barrier function. *Science* **2021**, *372* (6539), No. eabb1590.
- (21) Chassaing, B.; Koren, O.; Goodrich, J. K.; Poole, A. C.; Srinivasan, S.; Ley, R. E.; Gewirtz, A. T. Dietary emulsifiers impact the mouse gut microbiota promoting colitis and metabolic syndrome. *Nature* **2015**, *519* (7541), 92–96.
- (22) Buffie, C. G.; Bucci, V.; Stein, R. R.; McKenney, P. T.; Ling, L.; Gobourne, A.; No, D.; Liu, H.; Kinnebrew, M.; Viale, A.; et al. Precision microbiome reconstitution restores bile acid mediated resistance to *Clostridium difficile*. *Nature* **2015**, *517* (7533), 205–208.
- (23) Dodd, D.; Spitzer, M. H.; Van Treuren, W.; Merrill, B. D.; Hryckowian, A. J.; Higginbottom, S. K.; Le, A.; Cowan, T. M.; Nolan, G. P.; Fischbach, M. A.; et al. A gut bacterial pathway metabolizes aromatic amino acids into nine circulating metabolites. *Nature* **2017**, *551* (7682), 648–652.
- (24) Willing, B. P.; Dicksved, J.; Halfvarson, J.; Andersson, A. F.; Lucio, M.; Zheng, Z.; Järnerot, G.; Tysk, C.; Jansson, J. K.; Engstrand, L. A Pyrosequencing Study in Twins Shows That Gastrointestinal Microbial Profiles Vary With Inflammatory Bowel Disease Phenotypes. *Gastroenterology* **2010**, *139* (6), 1844–1854.e1.
- (25) Zhang, C.; Zhang, M.; Pang, X.; Zhao, Y.; Wang, L.; Zhao, L. Structural resilience of the gut microbiota in adult mice under high-fat dietary perturbations. *ISME Journal* **2012**, *6* (10), 1848–1857.
- (26) Ju, T.; Kong, J. Y.; Stothard, P.; Willing, B. P. Defining the role of *Parasutterella*, a previously uncharacterized member of the core gut microbiota. *ISME Journal* **2019**, *13* (6), 1520–1534.
- (27) Yilmaz, B.; Juillerat, P.; Öyäs, O.; Ramon, C.; Bravo, F. D.; Franc, Y.; Fournier, N.; Michetti, P.; Mueller, C.; Geuking, M.; et al. Microbial network disturbances in relapsing refractory Crohn's disease. *Nature Medicine* **2019**, *25* (2), 323–336.
- (28) Ning, L.; Zhou, Y.-L.; Sun, H.; Zhang, Y.; Shen, C.; Wang, Z.; Xuan, B.; Zhao, Y.; Ma, Y.; Yan, Y.; et al. Microbiome and metabolome features in inflammatory bowel disease via multi-omics integration analyses across cohorts. *Nat. Commun.* **2023**, *14* (1), 7135.
- (29) Ze, X.; Duncan, S. H.; Louis, P.; Flint, H. J. *Ruminococcus bromii* is a keystone species for the degradation of resistant starch in the human colon. *ISME Journal* **2012**, *6* (8), 1535–1543.
- (30) Eeckhaut, V.; Machiels, K.; Perrier, C.; Romero, C.; Maes, S.; Flahou, B.; Steppe, M.; Haesebrouck, F.; Sas, B.; Ducatelle, R.; et al. *Butyricoccus pullicaecorum* in inflammatory bowel disease. *Gut* **2013**, *62* (12), 1745–1752.
- (31) Devriese, S.; Eeckhaut, V.; Geirnaert, A.; Van den Bossche, L.; Hindryckx, P.; Van de Wiele, T.; Van Immerseel, F.; Ducatelle, R.; De Vos, M.; Laukens, D. Reduced Mucosa-associated *Butyricoccus* Activity in Patients with Ulcerative Colitis Correlates with Aberrant Claudin-1 Expression. *Journal of Crohn's and Colitis* **2017**, *11* (2), 229–236.
- (32) Chang, P. V.; Hao, L.; Offermanns, S.; Medzhitov, R. The microbial metabolite butyrate regulates intestinal macrophage function via histone deacetylase inhibition. *Proc. Natl. Acad. Sci. U. S. A.* **2014**, *111* (6), 2247–2252.
- (33) Sarkar, A.; Mitra, P.; Lahiri, A.; Das, T.; Sarkar, J.; Paul, S.; Chakrabarti, P. Butyrate limits inflammatory macrophage niche in NASH. *Cell Death & Disease* **2023**, *14* (5), 332.
- (34) Wang, Y.; Jiang, R.; Wu, Z.; Zhou, L.; Xu, J.; Huang, C.; Yang, L.; Zhu, B.; Yan, E.; Liu, C.; et al. Gut microbiota is involved in the antidepressant-like effect of (S)-norketamine in an inflammation model of depression. *Pharmacol. Biochem. Behav.* **2021**, *207*, 173226.
- (35) Chiaro, T. R.; Soto, R.; Zac Stephens, W.; Kubinak, J. L.; Petersen, C.; Gogokhia, L.; Bell, R.; Delgado, J. C.; Cox, J.; Voth, W.; et al. A member of the gut mycobiota modulates host purine metabolism exacerbating colitis in mice. *Science Translational Medicine* **2017**, *9* (380), No. eaaf9044.
- (36) Alexander, M.; Ang, Q. Y.; Nayak, R. R.; Bustion, A. E.; Sandy, M.; Zhang, B.; Upadhyay, V.; Pollard, K. S.; Lynch, S. V.; Turnbaugh, P. J. Human gut bacterial metabolism drives Th17 activation and colitis. *Cell Host & Microbe* **2022**, *30* (1), 17–30.e9.
- (37) Vich Vila, A.; Hu, S.; Andreu-Sánchez, S.; Collij, V.; Jansen, B. H.; Augustijn, H. E.; Bolte, L. A.; Ruigrok, R. A. A. A.; Abu-Ali, G.; Giallourakis, C.; et al. Faecal metabolome and its determinants in inflammatory bowel disease. *Gut* **2023**, *72* (8), 1472–1485.
- (38) Frascatani, R.; Mattogno, A.; Iannucci, A.; Marafini, I.; Monteleone, G. Reduced Taurine Serum Levels in Inflammatory Bowel Disease. *Nutrients* **2024**, *16* (11), 1593.
- (39) Marcinkiewicz, J.; Kontny, E. Taurine and inflammatory diseases. *Amino Acids* **2014**, *46* (1), 7–20.
- (40) Zheng, J.; Zhang, J.; Zhou, Y.; Zhang, D.; Guo, H.; Li, B.; Cui, S. Taurine Alleviates Experimental Colitis by Enhancing Intestinal Barrier Function and Inhibiting Inflammatory Response through TLR4/NF- $\kappa$ B Signaling. *J. Agric. Food Chem.* **2024**, *72* (21), 12119–12129.
- (41) Zelante, T.; Iannitti, Rossana G.; Cunha, C.; De Luca, A.; Giovannini, G.; Pieraccini, G.; Zecchi, R.; D'Angelo, C.; Massi-Benedetti, C.; Fallarino, F.; et al. Tryptophan Catabolites from Microbiota Engage Aryl Hydrocarbon Receptor and Balance Mucosal Reactivity via Interleukin-22. *Immunity* **2013**, *39* (2), 372–385.
- (42) Lamas, B.; Natividad, J. M.; Sokol, H. Aryl hydrocarbon receptor and intestinal immunity. *Mucosal Immunology* **2018**, *11* (4), 1024–1038.

(43) Alexeev, E. E.; Lanis, J. M.; Kao, D. J.; Campbell, E. L.; Kelly, C. J.; Battista, K. D.; Gerich, M. E.; Jenkins, B. R.; Walk, S. T.; Kominsky, D. J.; et al. Microbiota-Derived Indole Metabolites Promote Human and Murine Intestinal Homeostasis through Regulation of Interleukin-10 Receptor. *American Journal of Pathology* **2018**, *188* (5), 1183–1194.

(44) Zhang, J.; Zhang, R.; Chen, Y.; Guo, X.; Ren, Y.; Wang, M.; Li, X.; Huang, Z.; Zhu, W.; Yu, K. Indole-3-aldehyde Alleviates High-Fat Diet-Induced Gut Barrier Disruption by Increasing Intestinal Stem Cell Expansion. *J. Agric. Food Chem.* **2024**, *72* (34), 18930–18941.

(45) Scott, S. A.; Fu, J.; Chang, P. V. Microbial tryptophan metabolites regulate gut barrier function via the aryl hydrocarbon receptor. *Proc. Natl. Acad. Sci. U. S. A.* **2020**, *117* (32), 19376–19387.



CAS BIOFINDER DISCOVERY PLATFORM™

## CAS BIOFINDER HELPS YOU FIND YOUR NEXT BREAKTHROUGH FASTER

Navigate pathways, targets, and  
diseases with precision

Explore CAS BioFinder

